Lasers in Medical Science
https://doi.org/10.1007/s10103-022-03645-6

ORIGINAL ARTICLE

A novel 1726-nm laser system for safe and effective treatment of acne vulgaris

Matteo Giuseppe Scopelliti[1] · **Amogh Kothare**[1] · **Michael Karavitis**[1]

Received: 16 August 2022 / Accepted: 18 September 2022

Abstract
Selective photothermolysis of the sebaceous glands has the potential to be an effective alternative for treating acne vulgaris. However, the translation of this technique to clinical settings has been hindered by a lack of appropriate energy sources to target sebaceous glands, concerns surrounding safety, and treatment-related discomfort and downtime. In this work, we introduce the first FDA-approved system that combines a 1726-nm laser and efficient contact cooling to treat mild, moderate, and severe acne effectively while ensuring safety and minimal patient discomfort without adjunct pain mitigation techniques. Light transport and bioheat transfer simulations were performed to demonstrate the system's efficacy and selectivity. The resulting thermal damage to the skin and sebaceous glands was modeled using the Arrhenius kinetic model. Numerical simulations demonstrated that combining laser energy and optimal contact cooling could induce a significant temperature increase spatially limited to the sebaceous gland; this results in highly selective targeting and maximum damage to the sebaceous gland while preserving other skin structures. In vivo human facial skin histology results corroborated the simulation results. The studies reported here demonstrate that the presented 1726-nm laser system induces selective photothermolysis of the sebaceous gland, providing a safe and effective method for the treatment of acne vulgaris.

Keywords 1726-nm laser · Sebaceous glands · Acne · Laser acne treatment · Contact cooling

Introduction

Acne is the most common skin condition in the USA, affecting up to 50 million Americans yearly. In addition to discomfort and psychological distress, acne is associated with long-term effects, such as permanent skin scarring and poor self-esteem, ultimately resulting in significant psychosocial impact and lower quality of life [1–4].

Traditional acne treatments follow a well-established approach based on topical and systemic drugs [5]. While drug-based treatments for acne can be effective, they cause significant side effects ranging from skin irritation from topical therapies to teratogenicity and depression associated with systemic drugs like isotretinoin.

Recently, research efforts have been focused on developing effective alternative treatments that eliminate the need for drugs and rely, instead, on energy-based techniques. For example, it has been shown that radiofrequency (RF) devices and infrared light lasers can treat acne by targeting and destroying sebaceous glands, curbing excess sebum production, and, consequently, reducing *C. acnes* proliferation [6]. Infrared devices, such as 1320 and 1450 nm lasers, proved to be effective in treating acne but often caused intense pain and skin damage in treated subjects, a common limitation to some of these treatments [7].

The root cause of such undesirable effects can be identified in the lack of selectivity of those laser devices. Water is the most abundant component of soft biological tissue, and its absorption coefficient becomes significant in the infrared range. As a result, most of the energy delivered into the treatment region is absorbed by the water present in the tissue, causing a non-selective temperature rise that affects all the skin structures indiscriminately. During this process, sebaceous glands eventually become damaged by the increased temperature, but it comes at the price of intense discomfort and collateral skin damage for the patient.

A better strategy would be to selectively deliver light energy to specific target chromophores within the sebaceous gland having a higher absorption coefficient than

✉ Matteo Giuseppe Scopelliti
mscopelliti@cutera.com

[1] Cutera, Inc, Brisbane, CA, USA

Published online: 05 October 2022

water, resulting in selective damage with minimal alteration of the surrounding tissue. For example, the sebum in the glandular region is a viable endogenous target since it exhibits a narrow local absorption peak higher than water at 1726 nm, with a preferential absorption of 1.8:1 [8, 9], as shown in Fig. 1.

The concept of selective damage of the sebaceous glands is based on the theory of selective photothermolysis introduced in 1983 by Anderson and Parrish [10]. More recently, Sakamoto et al. successfully demonstrated that optical pulses with a wavelength of 1700–1720 nm could be used to destroy sebaceous glands in ex vivo human facial skin samples with minimal injury to other skin structures [11].

However, practical and technological challenges have hindered the application of selective photothermolysis for acne treatment in clinical settings. For this to happen, three primary requirements must be met: effectiveness, safety, and pain control.

A treatment is considered effective in achieving long-lasting acne clearing when a large temperature increase is induced inside the targeted glands for a long enough time, resulting in necrosis of the sebocytes. For this to happen, according to the theory of selective photothermolysis, the optical pulse width must be shorter than the target's thermal relaxation time (TRT), defined as the time required to lose 50% of the accumulated heat after energy is delivered. The mean TRT for human facial sebaceous glands is estimated to be around 60 ms [11]. Therefore, the laser system must be carefully designed to generate a significant and fast temperature rise inside the target, satisfying precise spectral and spatial requirements. First, the optical bandwidth of the laser should be narrow and centered at 1726 nm to match the selectivity peak of the sebum. Second, the beam diameter should be fine-tuned to provide large fluence values — inversely proportional to the squared beam radius — and penetration depth, proportional to the beam diameter [12].

At the same time, ensuring the patient's safety throughout the treatment is paramount. In this context, safety translates into the absence of severe or long-lasting adverse events potentially requiring medical intervention, such as skin burns and blistering, which result in permanent scarring. We have observed that such detrimental side effects can be prevented by keeping the temperature of the dermal–epidermal junction (DEJ) below 50 °C. However, considering that the preferential absorption of sebum is approximately two times higher than water, a substantial portion of the light energy is still absorbed by the epidermis and dermis, potentially resulting in temperature peaks higher than 50 °C. As a result, additional cooling strategies are required to preserve the integrity of the skin and achieve the thermal damage selectivity necessary for a safe treatment.

The third requirement, especially significant in clinical settings, is minimizing the discomfort experienced by patients during treatment. In fact, a patient may be reluctant to undergo or complete a painful session, despite the promises of safety and effectiveness. This consideration is particularly valid for treatments based on thermal ablation or photothermolysis since heat stimulates the pain receptors in the skin. It has been demonstrated that the typical heat pain threshold for skin is between 42 and 45 °C, but it is also affected by the duration of heat exposure [13, 14].

To sum up, the successful application of selective photothermolysis in clinical settings must ensure effectiveness and safety while managing the pain experienced by the patients. These requirements can be satisfied by finely balancing the heating and cooling of the treated skin. In this paper, we introduce a

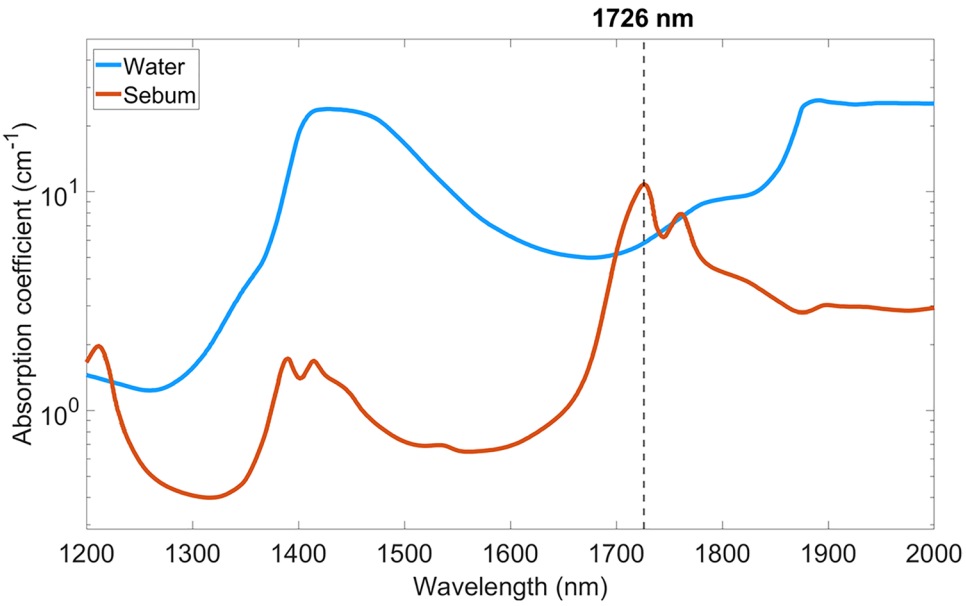

Fig. 1 Measured absorption coefficient (μ_a) of water and sebum in the mid-infrared range [8]

novel system based on a 1726-nm laser, specifically designed to precisely target sebaceous glands. In addition, a highly efficient contact cooling system integrated into the system's handpiece protects the skin from hyperthermia-induced side effects, ensuring safety and pain control throughout the treatment.

Methods

Laser system

The core of the laser system is a fiber-coupled 100-Watt diode laser emitting light at $\lambda = 1726$ nm. Laser pulses (up to 50 ms) are delivered through a custom-designed handpiece, featuring an efficient contact cooling system deploying a sapphire window that is actively cooled between 0 and 5 °C. Compared to other traditional temperature-control alternatives for clinical applications, contact cooling provides faster and more localized heat extraction than convective methods [15] and does not cause cryonecrosis, a side effect sometimes observed with cryogen spray cooling [16]. Furthermore, the skin compression resulting from pressing the sapphire window onto the skin brings deeper targets closer to the output of the handpiece, reducing the physical thickness of the interposed tissue and increasing the fraction of energy reaching buried glands [16].

The main limitation of contact cooling is the perfect-contact requirement of the clear aperture of the sapphire, meaning that optimal heat extraction can be achieved only when the entire sapphire window area is in direct contact with the skin surface. For this reason, contact and pressure sensing technology is embedded on the tip of the system's handpiece to prevent laser-firing unless the sapphire window makes adequate contact and is uniformly pressed onto the skin.

Each treatment session includes multiple applications over the area affected by acne, and each application consists of three phases: pre-cooling, energy delivery accompanied with parallel cooling, and post-cooling. The pre-cooling phase starts when the cooling window is applied to the skin and ends when the laser pulse is fired. This first step is designed to lower the initial temperature of the epidermis, dermis, and DEJ, limiting the temperature rise and preventing collateral thermal damage.

Laser energy is delivered to the pre-cooled area through the sapphire window, which continues to cool the skin surface during energy delivery. The post-cooling phase starts right after the laser pulse is fired and the energy is delivered to the treatment region. This phase lasts long enough to offset the potentially harmful thermal blooming when the heat accumulated inside the gland is quickly released to the surrounding tissue. Moreover, post-cooling contributes to quickly restoring physiological skin temperature, minimizing the duration of pain stimuli.

Numerical modeling

Light transport and heat transfer numerical models were implemented to characterize the operating parameters of the presented system and the resulting thermal damage. Several assumptions were made to reduce the computational cost of such models, detailed in the subsequent sections below. Therefore, the presented results are not intended to be exact but to provide a good understanding of the thermal distribution and damage to the tissue for different combinations of parameters.

Light transport

The fluence resulting from the interaction of the laser beam with skin tissue and the sebaceous gland was modeled using an open-source Monte Carlo light transport simulator (Monte Carlo eXtreme v2020, http://mcx.space). The 3D simulation domain was implemented as a 10 mm × 10 mm × 5 mm homogeneous skin volume with a voxel size of 10 µm × 10 µm × 10 µm. A sebaceous gland, modeled as a simple sphere with a diameter of 0.24 mm, was positioned 0.8 mm deep into the tissue, aligned with the center of a 3-mm wide circular laser beam with a uniform profile (top-hat) incident on the skin surface.

The refractive index and the anisotropy factor of the tissue at the wavelength of 1726 nm were set to $n = 1.363$ and $g = 0.9$, respectively. Absorption coefficients μ_a and scattering coefficients μ_s for skin and human fat used to approximate the optical properties of the sebum are listed in Table 1 [8, 17, 18].

Bioheat transfer

The fluence data obtained from the Monte Carlo simulations were used as an input for a finite element (FE) model (COMSOL Multiphysics 6.0, COMSOL Inc., USA) to estimate the temperature rise within the target tissue.

A schematic view of the simulation domain is reported in Fig. 2, showing the actively cooled sapphire window placed on the top surface of the skin. A 2-layer model that includes epidermal and dermal layers was used to represent the skin,

Table 1 Optical parameters used for the Monte Carlo light transport simulations

Component	Absorption coefficient μa (mm^{-1})	Scattering coefficient μs (mm^{-1})	Anisotropy factor g	Refractive index n
Skin	0.59	8.5	0.9	1.363
Sebaceous gland (fat)	1.062	8.0	0.9	1.363

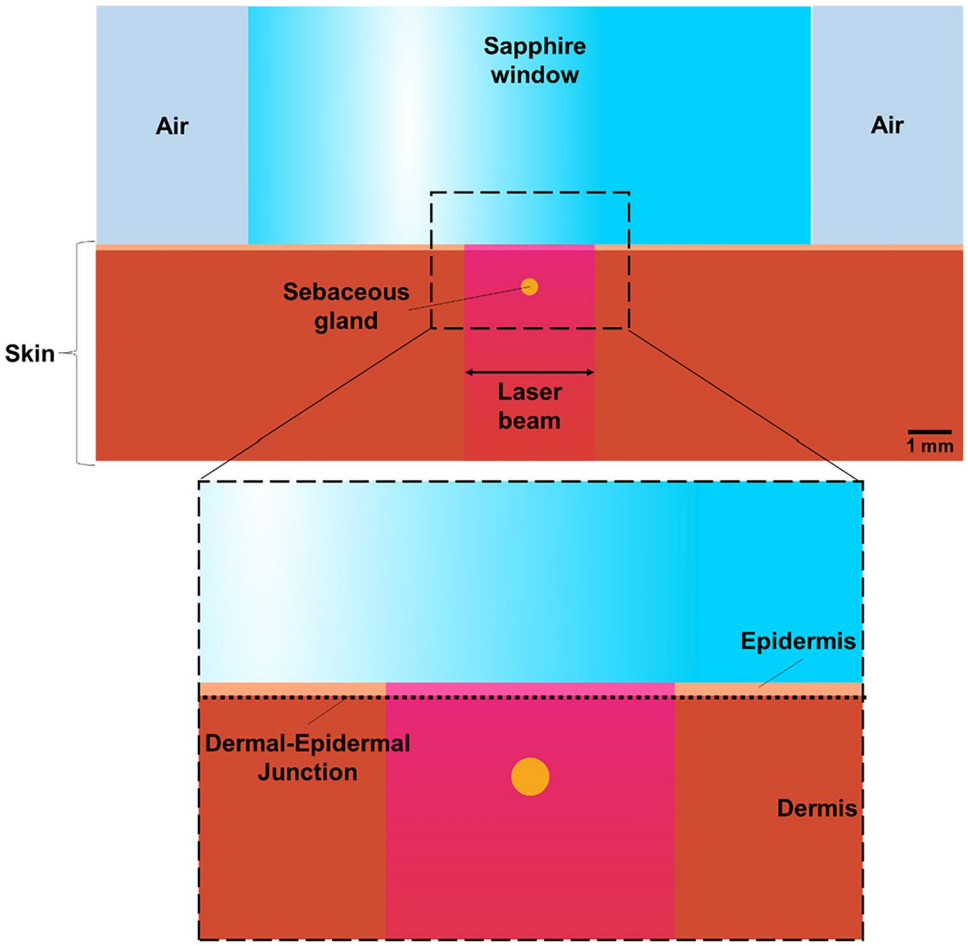

Fig. 2 Schematic representation of the bioheat transfer simulation domain

allowing for tracking the temperature evolution at the dermal–epidermal junction (inset of Fig. 2) is critical to assess the safety of the treatment.

In this model, a single laser pulse was emitted from the center of the sapphire window, traveling through the skin layers and the sebaceous gland, modeled as a sphere of human fat at a depth of 0.8 mm. The thermal parameters used for the simulations are reported in Table 2 [12, 19, 20].

The spatiotemporal temperature distribution within the simulation domain was calculated by numerical solution of the Pennes' bioheat transfer equation.

Table 2 Thermal parameters used for the bioheat transfer numerical simulations

Component	Thermal conductivity k (W/(m·K))	Density ρ (kg/m^3)	Specific heat c_p (J/(kg·K))
Sapphire	23.1	3980	761
Epidermis	0.5	1200	3600
Dermis	0.53	1200	3800
Fat (sebum)	0.21	911	2348

Thermal damage estimation

The traditional Arrhenius kinetic model was used to estimate the thermal tissue damage caused by hyperthermia as a function of heating time and temperature [21]. The dimensionless damage parameter Ω is defined as the logarithm of the ratio of the native tissue concentration before ($C(0)$) and after ($C(\tau)$) the tissue heating, is calculated as:

$$\Omega(\tau) = ln\left(\frac{C(0)}{C(\tau)}\right) = \int_0^\tau Ae^{\left[\frac{-E_a}{RT(t)}\right]}dt \quad (1)$$

where τ is the total heating time, A is the pre-exponential frequency factor, E_a is the activation energy, R is the universal gas constant, and $T(t)$ is the absolute temperature at time t.

Table 3 Arrhenius model parameters used for estimating the thermal damage

Tissue temperature	Frequency factor A (s^{-1})	Activation energy Ea (J/mol)
$T \leq 53$ °C	8.82×10^{94}	6.03×10^5
$T > 53$ °C	1.297×10^{31}	2.04×10^5

The Arrhenius parameters used in our model are reported in Table 3 [21, 22].

Results

Light transport

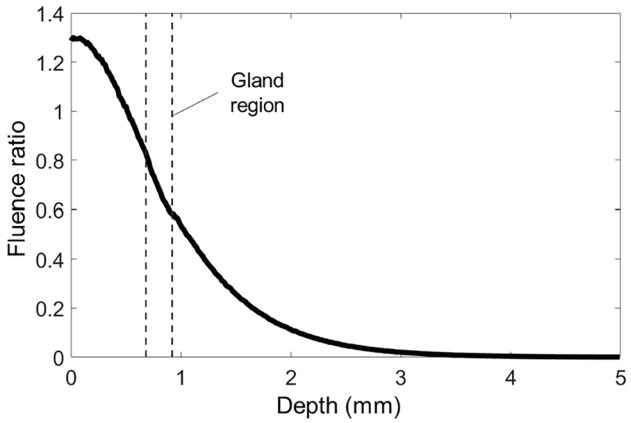

Fig. 3 Simulated fluence ratio versus tissue depth measured at the center of a 3-mm wide laser beam

Monte Carlo simulation results for laser light transport at 1726 nm through the skin were analyzed to estimate the fluence ratio, defined as:

$$F_{ratio}(z) = \frac{F(x,y,z)}{F_0(x,y)} \tag{2}$$

where F_0 represents the initial fluence measured at the output of the handpiece. Figure 3 reports the fluence ratio measured at the center of the laser beam as a function of depth, showing that 60–80% of the initial fluence is delivered to the targeted gland.

Bioheat transfer

Effect of pre-cooling phase

The FE model was used to estimate the effect of the pre-cooling phase, defined as the time between applying the cooling window on the skin and the moment the laser pulse is fired.

The sapphire window temperature in the FE model was set to 2 °C. Domain and boundary thermal probes were added at the dermal–epidermal junction (T_{DEJ}), sebaceous gland (T_G), and the upper region of the dermis (T_D), as schematically shown in Fig. 4a. Such probes were used to measure and track the temporal evolution of average temperatures at these critical locations, as reported in Fig. 4b. The simulation results indicate that the average temperature at the DEJ decays quickly within 0.5 s, which is expected considering the proximity to the cooling system. In contrast, the average temperatures of the dermis and gland present an expected cooling delay since they are farther away from the sapphire window.

The pre-cooling phase must ensure the maximum cooling of the DEJ and dermis to prevent side effects caused by hyperthermia and reduce the perceived pain during the treatment. At the same time, the cooldown of the gland should be minimal to avoid affecting the amount of thermal damage caused by the laser beam.

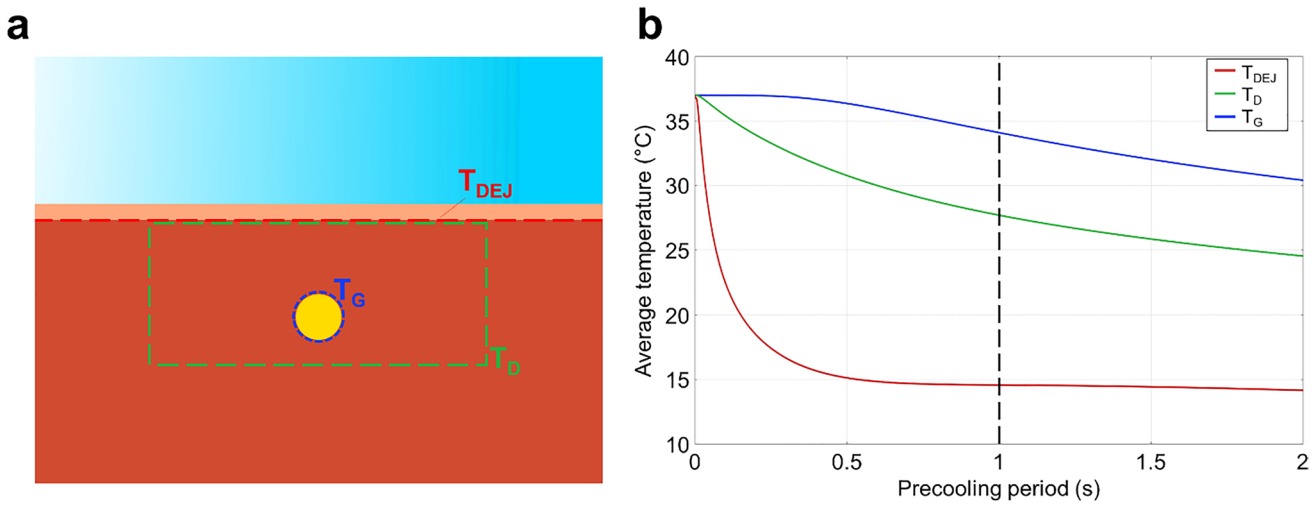

Fig. 4 **a** Schematic illustration of the domain and boundary probes used to track the temperature at the dermal–epidermal junction (T_{DEJ}), inside the gland (T_G), and in the dermal region surrounding it (T_D). **b** Average probe's temperatures plotted versus the pre-cooling period duration

Simulation results show that a pre-cooling period of 1 s at a temperature of 2 °C (dashed line in Fig. 4b) meets both the requirements, as the T_{DEJ} reaches an average temperature of 14.6 °C, and T_D is reduced by 9.3 °C. Moreover, T_G shows just a minor variation (~ 3 °C) compared to its initial value.

Laser-tissue interaction

Bioheat transfer simulations were performed to evaluate the thermal damage caused by the combination of heating and cooling provided by the system on skin and sebaceous gland.

The fluence ratio profile shown in Fig. 3 was imported into the bioheat transfer model, and the initial fluence was set to $F_0 = 20.5$ J/cm^2, delivered through a single laser pulse. Next, the cooling temperature was set to 2 °C, and the contact cooling system was modeled as continuously active starting at 1 s before the laser pulse (pre-cooling) to 2 s after (post-cooling).

A 2D cross-section of the temperature distribution within the skin and sebaceous gland immediately after the pulse (Fig. 5a) shows that the rise in temperature within the gland is significantly larger than in any other region irradiated by the same laser pulse. The plots in Fig. 5b illustrate the temporal evolution of the maximum temperatures measured by the probes during the entire application. It is possible to observe that the maximum temperature at the dermal–epidermal junction never exceeds the safety threshold ($T_{DEJ} < 50$ °C). In contrast, the maximum temperature inside the gland rises quickly up to 98.2 °C. Moreover, the maximum temperature of the dermis falls below the pain threshold by the end of the post-cooling period, suggesting an effective reduction of the discomfort experienced by the patients.

Figure 5c shows that the peak difference between the gland's and dermis's maximum temperature is $\Delta T_{DG} = 32.8$ °C, further corroborating the selectivity of the thermal damage, primarily confined to the target structure.

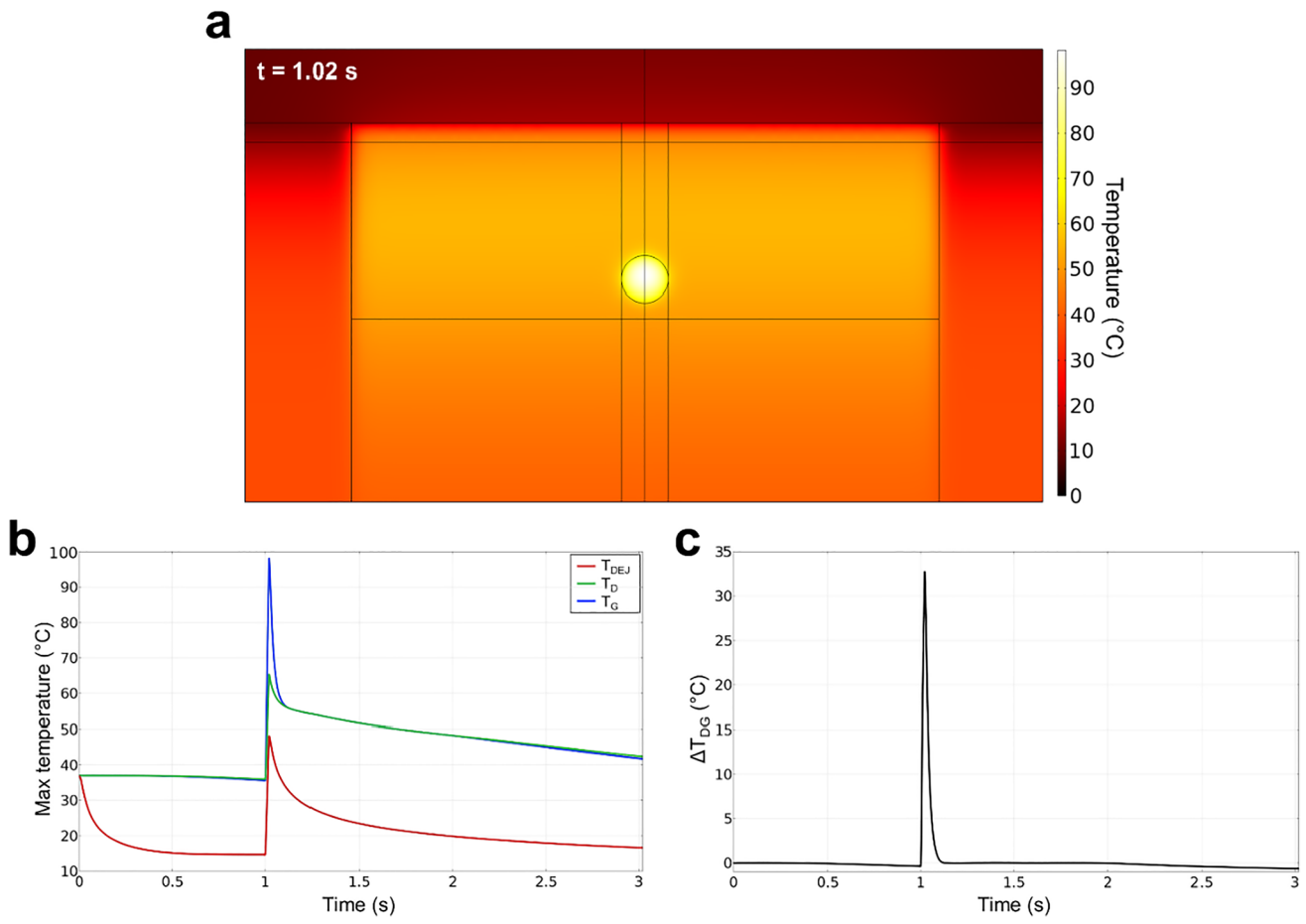

Fig. 5 **a** 2D cross-section of the temperature distribution within the skin and sebaceous gland immediately after the laser pulse is delivered. **b** Maximum temperatures tracked over time by the probes shown in Fig. 4a. **c** Difference between the maximum temperatures of gland and dermis, showing a thermal selectivity peak right after the laser pulse (ΔT_{DG})

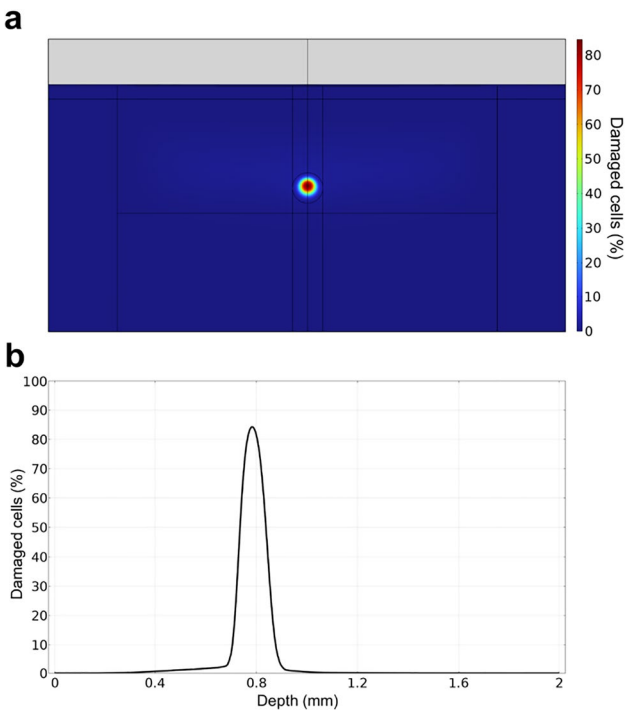

Fig. 6 **a** Cross-section of the skin model, showing that thermal damage selectively affects cells within the glandular region. **b** Highest percentage of damaged cells at each depth

Thermal damage

The percentage of cells damaged by laser-induced hyperthermia was estimated by using the following equation derived from Eq. 1:

$$\text{Damaged cells } (\%) = \left(1 - e^{(-\Omega)}\right) \times 100 \tag{3}$$

The 2D map reported in Fig. 6a shows the spatial distribution of damaged cells after a single application, exhibiting an expected correlation with the temperature distribution shown in Fig. 5a. The plot in Fig. 6b reports the maximum percentage of damaged cells at each depth, showing a peak value of 84.3% inside the sebaceous gland, which results in irreversible necrosis of the sebocytes. Additionally, the negligible fraction of damaged cells (< 3%) outside the glandular region suggests insignificant collateral damage to the dermis and epidermis.

In vivo tissue response to laser treatment

Findings of the finite element modeling were evaluated in postoperative histological examination of an in vivo human facial skin model. Human facial skin around the ear was exposed to therapeutic energy settings determined by the model. The treated skin was excised 5 days post laser exposure, and the corresponding microscopic sections are shown in Fig. 7a-b, with a magnification of 40 × and 200 ×, respectively. Epidermal tissue showed no signs of continuing inflammation 5 days post-treatment during the biopsy. Total necrosis of the sebaceous gland was observed with complete sparing of the epidermis and follicular epithelium. The damage to the sebaceous gland was observed across the length of the gland.

Figure 8 shows the photos taken from an IRB-approved study of a skin type III patient affected by moderate acne, before and after a cycle of three treatments with the presented system. Comparing the pictures, it is possible to appreciate the efficacy and the long-lasting effects induced by the selective photothermolysis of the sebaceous glands.

Conclusion

In this work, we presented a novel energy-based system for treating acne vulgaris through selective photothermolysis of the sebaceous gland, aimed at curbing excess sebum production and *C. acne* proliferation.

Numerical simulations for light transport and bioheat transfer, based on Monte Carlo methods and Pennes' equation, respectively, were performed to identify suitable treatment parameters and demonstrate that selective photothermolysis of the sebaceous gland could be safely achieved. Simulation results showed that a 1-s pre-cooling period is

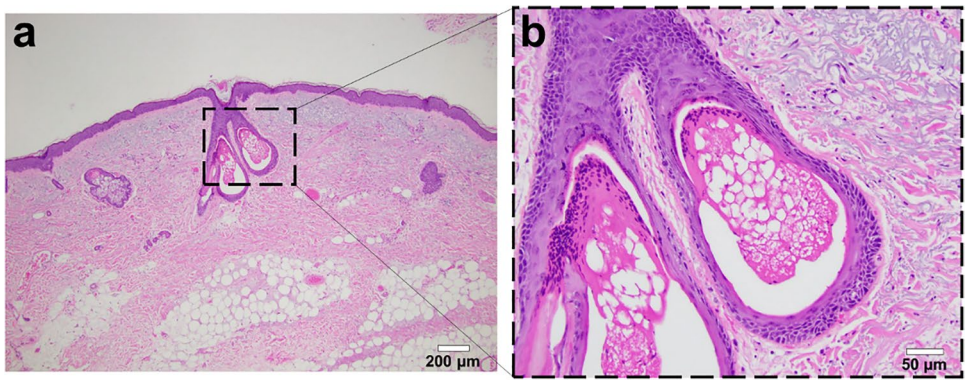

Fig. 7 **a** Histology of treated human facial skin after treatment. **b** Closer view of the damaged sebaceous glands

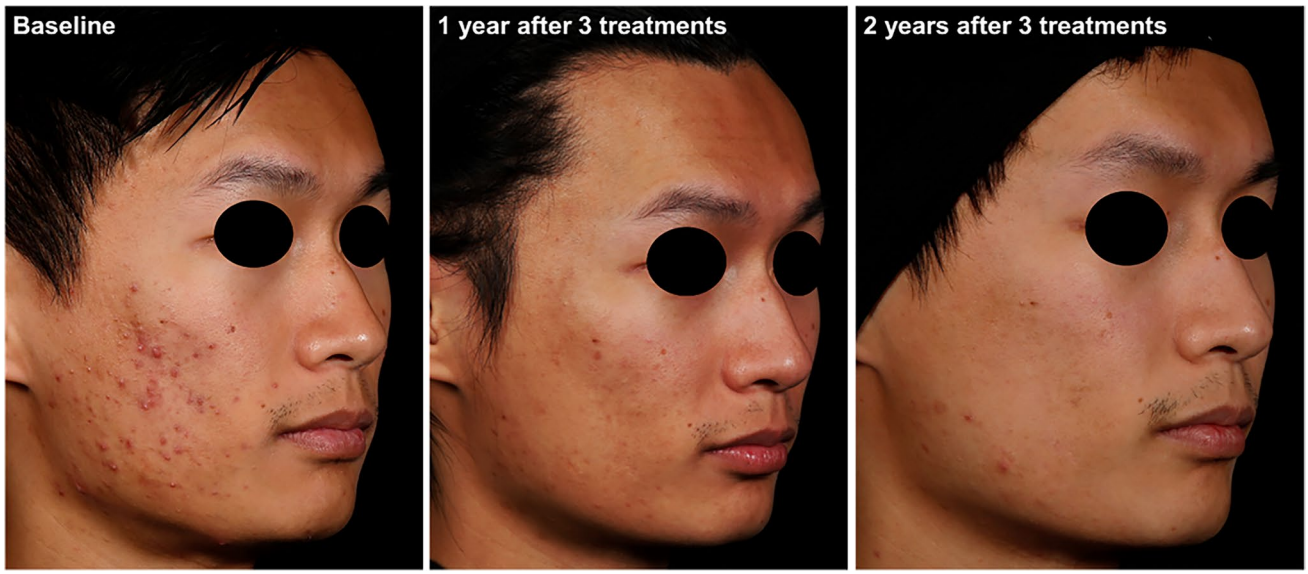

Fig. 8 Long-lasting acne clearing of a patient treated with the presented system

sufficient to protect the skin without significantly affecting the temperature of the sebaceous gland, and a single laser pulse with an initial fluence of $F_0 = 20.5$ J/cm^2 can induce a significant temperature increase within the gland, selectively damaging sebocytes. Furthermore, thanks to the contact cooling system, the temperature of the dermal–epidermal junction does not exceed the critical value of 50 °C when light energy is delivered to the tissue, indicating serious side effects like blistering and skin burning are successfully prevented. Finally, the 2-s post-cooling phase effectively contrasts the thermal blooming after the energy is delivered to the gland and quickly lowers the dermis's temperature below the pain threshold (42–45°), reducing the discomfort experienced by the patients.

In conclusion, the presented system can effectively induce selective photothermolysis of the sebaceous gland while preventing collateral damage to the dermis and epidermis and managing patients' discomfort. Results from clinical trials will be published in future manuscripts.

Funding This study was funded by Cutera, Inc., USA.

Declarations

Ethics approval and consent to participate Clinical data presented in this article was collected under an IRB-approved study (C-19-AC-01). The Institutional Review Board approving this study was IntegReview, LLC, Austin, USA. All contents adhered to the tenets of the Declaration of Helsinki. The participant has consented to the publication of the images in Fig. 8.

Competing interests Matteo Giuseppe Scopelliti, Amogh Kothare, and Michael Karavitis are employees of Cutera, Inc., USA.

References

1. Koo J (1995) The psychosocial impact of acne: patients' perceptions. J Am Acad Dermatol 32(5 Pt 3):S26-30. https://doi.org/10.1016/0190-9622(95)90417-4
2. Uhlenhake E, Yentzer BA, Feldman SR (2010) Acne vulgaris and depression: a retrospective examination. J Cosmet Dermatol 9(1):59–63. https://doi.org/10.1111/j.1473-2165.2010.00478.x
3. Dunn LK, O'Neill JL, Feldman SR (2011) Acne in adolescents: quality of life, self-esteem, mood, and psychological disorders. Dermatol Online J 17(1):1
4. Smithard A, Glazebrook C, Williams H (2001) Acne prevalence, knowledge about acne and psychological morbidity in mid-adolescence: a community-based study. Br J Dermatol 145(2):274–279
5. Zaenglein AL et al (2016) Guidelines of care for the management of acne vulgaris. J Am Acad Dermatol 74(5):945–73 e33. https://doi.org/10.1016/j.jaad.2015.12.037
6. Rotunda AM, Bhupathy AR, Rohrer TE (2004) The new age of acne therapy: light, lasers, and radiofrequency. J Cosmet Laser Ther 6(4):191–200
7. Hædersdal M, Togsverd-Bo K, Wulf H (2008) Evidence-based review of lasers, light sources and photodynamic therapy in the treatment of acne vulgaris. J Eur Acad Dermatol Venereol 22(3):267–278. https://doi.org/10.1111/j.1468-3083.2007.02503.x
8. Ezerskaia A, Pereira SF, Urbach HP, Varghese B (2018) Depth resolved quantitative profiling of stratum corneum lipids and water content using short-wave infrared spectroscopy. In Zeng H, Choi B (eds) Photonics in Dermatology and Plastic Surgery 2018 (Vol. 10467). [104670R] (Progress in Biomedical Optics and Imaging - Proceedings of SPIE; Vol. 10467). SPIE. https://doi.org/10.1117/12.2291896
9. Ezerskaia A et al (2016) Quantitative and simultaneous non-invasive measurement of skin hydration and sebum levels. Biomed Opt Express 7(6):2311–2320. https://doi.org/10.1364/BOE.7.002311
10. Anderson RR, Parrish JA (1983) Selective photothermolysis: precise microsurgery by selective absorption of pulsed radiation. Science 220(4596):524–527. https://doi.org/10.1126/science.6836297

11. Sakamoto FH et al (2012) Selective photothermolysis to target sebaceous glands: theoretical estimation of parameters and preliminary results using a free electron laser. Lasers Surg Med 44(2):175–183. https://doi.org/10.1002/lsm.21132
12. Ash C et al (2017) Effect of wavelength and beam width on penetration in light-tissue interaction using computational methods. Lasers Med Sci 32(8):1909–1918. https://doi.org/10.1007/s10103-017-2317-4
13. Pertovaara A, T Kauppila M Hämäläinen, (1996) *Influence of skin temperature on heat pain threshold in humans.* Experimental Brain Research 107(3). https://doi.org/10.1007/bf00230429.
14. Nielsen J, Arendt-Nielsen L (1998) The influence of rate of temperature change and peak stimulus duration on pain intensity and quality. Somatosens Mot Res 15(3):220–229. https://doi.org/10.1080/08990229870781
15. Nelson JS, Majaron B, Kelly KM (2000) Active skin cooling in conjunction with laser dermatologic surgery. Semin Cutan Med Surg 19(4):253–266. https://doi.org/10.1053/sder.2000.18365
16. Das A, Sarda A, De A (2016) Cooling devices in laser therapy. J Cutan Aesthet Surg 9(4):215–219. https://doi.org/10.4103/0974-2077.197028
17. Troy TL, Thennadil SN (2001) Optical properties of human skin in the near infrared wavelength range of 1000 to 2200 nm. J Biomed Opt 6(2):167–176. https://doi.org/10.1117/1.1344191
18. Jacques SL (2013) Optical properties of biological tissues: a review. Phys Med Biol 58(11):R37-61. https://doi.org/10.1088/0031-9155/58/11/R37
19. Princeton Scientific Corp. *Aluminium oxide — sapphire for VIS and IR-range*. Available from: https://princetonscientific.com/materials/optical-components/aluminium-oxide-sapphire-vis-ir-range/. Accessed 22 February 2022
20. Hasgall PA, D.G.F., Baumgartner C, Neufeld E, Lloyd B, Gosselin MC, Payne D, Klingenböck A, Kuster N,. *IT'IS database for thermal and electromagnetic parameters of biological tissues*. Feb 22, 2022; Version 4.1:[Available from: itis.swiss/database.
21. Pearce JA (2013) Comparative analysis of mathematical models of cell death and thermal damage processes. Int J Hyperthermia 29(4):262–80. https://doi.org/10.3109/02656736.2013.786140
22. Diller KR, Valvano JW, Pearce JA (2000) Bioheat transfer. The CRC Handb Therm Eng 4:114–187